

Recombinant Spider Silk Protein and Delignified Wood Form a Strong Adhesive System

Laura Lemetti, Jennifer Tersteegen, Juuso Sammaljärvi, A. Sesilja Aranko, and Markus B. Linder*

Cite This: *ACS Sustainable Chem. Eng.* 2022, 10, 552–561

Read Online

ACCESS |



Metrics & More



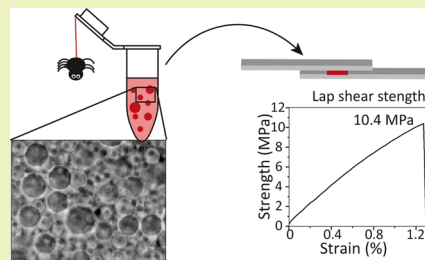
Article Recommendations



Supporting Information

ABSTRACT: For developing novel fully biological materials, a central question is how we can utilize natural components in combination with biomimetic strategies in ways that both allow feasible processing and high performance. Within this development, adhesives play a central role. Here, we have combined two of nature's excellent materials, silk and cellulose, to function as an adhesive system. As an initial step in processing, wood was delignified. Without lignin, the essential microstructure and alignment of the wood remain, giving a strong scaffold that is versatile to process further. A recombinant spider silk protein was used as a fully biological and water-based adhesive. The adhesive strength was excellent with an average value of 6.7 MPa, with a maximum value of up to 10 MPa. Samples of different strengths showed characteristic features, with high tear-outs for weaker samples and only little tear-out for strong samples. As references, bovine serum albumin and starch were used. Based on the combined data, we propose an overall model for the system and highlight how multiple variables affect performance. Adhesives, in particular, biobased ones, must be developed to be compatible with the overall adherend system for suitable infiltration and so that their mechanical properties match the adherend. The engineering of proteins gives an unmatched potential for designing adhesive systems that additionally have desired properties such as being fully water-based, biologically produced, and renewable.

KEYWORDS: cellulose, protein engineering, cellulose-binding domain, lap shear strength, bovine serum albumin, *Araneus diadematus*, adhesion, amino acid analysis



INTRODUCTION

There is currently a strong drive to develop new sustainable materials. For finding inspiration and new components, it is relevant to turn to the abundance of excellent materials found in nature. We should examine the use of natural components when developing a new material solution to enable sustainable and efficient use of raw materials. For wider use, we need not only to learn from natural materials but also to apply biological materials in new ways that are compatible with industrial processing.^{1,2}

Here, we have focused on a new way of combining two well-known and excellent materials, cellulose and silk, into an adhesive system taking advantage of the benefits of both materials. Cellulose is overall highly abundant and on the molecular level, it is an extremely strong and versatile polymer.^{3,4} To explore new processing methods for broader use of wood, including ways for recycling wood scrap or smaller pieces, there has recently been much interest in processes involving delignification.⁵ In delignification, the lignin fraction of wood is dissolved by immersion in an oxidizing bath in acidic conditions, leaving only cellulose and residual hemicellulose (Scheme 1A). The microstructure of the cell walls remains, and the loosened cellulose can be compressed and dried again. Excellent mechanical properties can be obtained since the optimal packing and close native

alignment of cellulose fibrils are not disturbed.⁶ A further advantage is that the moldability of the wet cellulose allows it to be compressed into different shapes. For widening the range of use of delignified cellulose, one important development will be to find suitable adhesives that are compatible with its processing steps. New adhesives will allow combining individual pieces together into larger assemblies and could widen the range of use of delignified cellulose.⁵

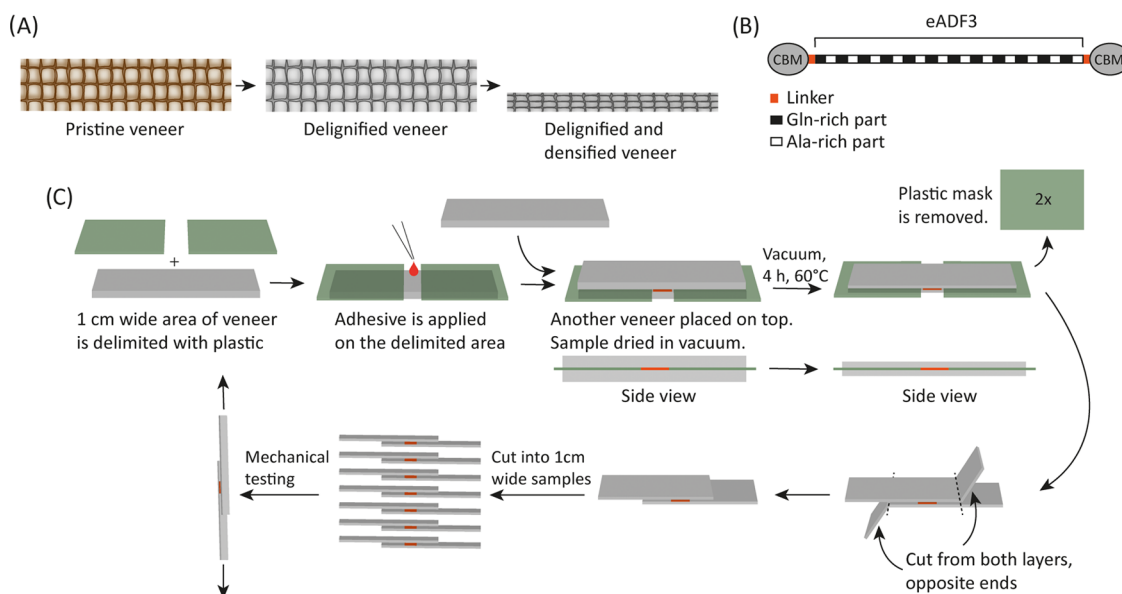
For constructing samples, we applied a drying technique utilizing vacuum suction.⁷ The system has the benefit that it allows the use of wet, never-dried cellulose. Drying in vacuum also enables molding the material during the gluing process.⁸ Therefore, in adhesive systems for delignified cellulose, the processing in a wet state is particularly important. As a practical consideration, drying the cellulose in between delignification and bonding would be an unnecessary step. Also, the drying of cellulose would result in aggregation of fibers, which means that the open ultrastructure formed as a result of the

Received: October 15, 2021

Revised: December 13, 2021

Published: December 22, 2021



Scheme 1. Components and Preparation of the Adhesive System^a

^a(A) Delignification and densification steps, (B) overall structure of the CBM-eADF3-CBM protein used in this study as an adhesive, and (C) sample preparation for lap shear testing. Gluing of two sheets of veneer gave a set of seven sample strips for mechanical testing.

delignification would collapse, hampering the shaping and molding processes.⁹ Therefore, an important consideration for an adhesive for the delignified cellulose is whether it can function in an aqueous processing environment.

Silk proteins form a large and diverse family of proteins and are particularly interesting as biological adhesives. A large potential lies in the use of structurally engineered variants and production by recombinant expression systems. This would open a route toward sustainable and industrially scalable manufacturing. In addition to the well-known *Bombyx mori* silk and spider dragline silks, many organisms produce silk proteins for various adhesive or structural purposes.¹⁰ Overall, high toughness, cohesiveness, and adhesiveness are associated with many variants of silks.^{11–13} We worked here with a highly engineered variant of the spider *Araneus diadematus* ADF3-protein, called eADF3, which was one of the first spider silks that was produced by recombinant means in *Escherichia coli*.¹⁴ The eADF3 sequence itself can be in a random coil form containing α -helical structures when freshly prepared. As a step in its assembly process, it can undergo liquid–liquid phase separation (LLPS), forming a condensed phase of protein that can then further solidify, which leads to an increased β -sheet content.¹⁵ More generally, LLPS has been suggested as an important intermediate step for several biological adhesives.¹⁶ Much of our understanding of LLPS comes from studies of adhesive mussel foot proteins.¹⁷

The structure of native spider silks includes folded modules in both termini of the disordered middle sequence. In the native protein structure, these terminal modules induce dimerization.^{18,19} Molecular structural engineering of silks, such as the module organization, allows introducing new functional properties. The variant CBM-eADF3-CBM that we used in the current work was engineered to have cellulose-binding modules (CBMs) as terminal modules (Scheme 1B).²⁰ The CBMs show an affinity for cellulose and are naturally found, for example, to function as attachment modules in enzymes that degrade cellulose.²¹ In preliminary work, we identified that the combination of modules provides an

adhesive function that none of the components by themselves have.^{15,22} Testing the fusion of CBMs without the middle silk module or the silk part alone was inferior to the full combination CBM-eADF3-CBM. Subsequent work involving computer modeling suggested that the overall triblock modular structure functions differently than the individual parts by promoting intramolecular interactions between protein molecules.²³ It was suggested that the reason for this is that the terminal modules show dimerization interactions that work in synergy with the intermolecular interactions that the silk sequences show.²⁴ In particular, the overall architecture affected the way in which condensates were formed and the internal structuring of the condensates into a bicontinuous network.²³ The observed internal structuring indicates that the silk proteins are entangled and interact within the condensed phase. In general, internal network structuring has a significant role in polymer adhesion.²⁵ However, the previously tested adhesive systems were based on paper-like materials and were overall not very strong due to the structurally relatively weak adherend.²²

In this work, as our experimental setup, we studied the lap shear strength of delignified wood veneers with the engineered CBM-eADF3-CBM as an adhesive. As a general reference adhesive, we chose bovine serum albumin (BSA) because it has widely been used as a protein adhesive in the past. It functions remarkably well and has even shown better performance than some types of recombinant silk proteins.²⁶ Therefore, BSA is useful as a general benchmark reference that is also easily reproducible across the research community. As another reference adhesive, we used starch as it has been previously suggested as an adhesive for delignified wood.²⁷

EXPERIMENTAL SECTION

Protein Expression in *E. coli* and Purification. The engineered silk protein CBM-eADF3-CBM having a triblock structure was made as previously described.²⁰ Briefly, the modified ADF3 dragline sequence (eADF3) from *A. diadematus* was used as a middle block, to which folded CBM-terminal groups were fused by short linkers (2

kDa). CBM sequences were from the CipA-scaffoldin subunit from *Clostridium thermocellum*. The molecular weight of CBM-eADF3-CBM was 85 288 Da.

For protein expression, an EnPresso B500 medium was used. After breaking of cells, purification of the recombinantly expressed protein was carried out by heating the crude extract to 70 °C for 30 min followed by centrifugation to remove the precipitated impurities. The protein-containing supernatant was collected and gel-filtrated into deionized water using EconoPac 10 DG columns (Bio-Rad).

Delignification of Spruce Veneer. Spruce timber was obtained from a local lumberyard, Espoo, Finland. Veneer slices with dimensions of 3 mm × 100 mm × 800 mm were cut radially from the timber and used for delignification. A mixture of glacial acetic acid (Fisher Scientific) and 35% hydrogen peroxide (Fisher Scientific) in a 1:1 volume ratio at 80 °C for 6 h was used to remove lignin according to Frey et al.⁵ Treated veneer was washed with deionized water for 1 week to neutralize the pH. The water was exchanged daily. Wet veneer was used for the preparation of lap shear samples.

Preparation of Adhesives. Protein samples were prepared by concentrating them until LLPS was observed. Concentrating was carried out with Vivaspin centrifugal concentrators (Sartorius, 30 kDa cutoff), and the concentration of the protein solution was determined from band intensities on Coomassie-stained SDS-PAGE using protein standards. An immobilized metal affinity chromatography purified CBM-eADF3-CBM was used as a standard reference for concentration determination. The concentration of the reference was determined by amino acid analysis. The comparison of band intensities was carried out with ImageJ software. The presence of phase separation was always confirmed with optical microscopy (Zeiss Axio Vert A1 with AxioCam 503 color camera).

BSA and starch were used as controls in adhesive tests. BSA was dissolved in deionized water to a 80 mg mL⁻¹ concentration and was then used as such for lap shear sample preparation. Starch was mixed with deionized water to yield a 16.5 wt % solution. Starch formed a thick paste with water, and it was mixed with a magnetic stirrer overnight to obtain a homogeneous mixture.

Preparation of Lap Shear Samples. Both ends of a delignified veneer were masked with plastic sheets so that a 1 cm wide area was exposed in the middle (Scheme 1C.). The adhesive was applied on this 1 × 8 cm² area. A total of 700 μL of protein (14 mg or 70 mg silk, or 56 mg BSA) or 0.3 g of starch was used to prepare the lap shear sample. Another layer of veneer was then placed on top of the first one. Samples were dried in vacuum at 65 °C for 4 h and then equilibrated at 65% relative humidity and 20 °C for 3 days prior to measuring. Strips for tensile testing were cut before measuring.

Lap Shear Measurements. Before measuring, the sample was trimmed by shortening one end of each veneer sheet from opposite sides to obtain a suitable lap shear sample geometry, as shown in Scheme 1C. Samples were cut into strips (10 mm wide and 100 mm long), with wood grains running parallel to the long dimension. Typically, one sheet gave seven strips.

Lap shear measurements were performed with a Zwick MTS, 20 kN load cell, and a 10 mm min⁻¹ cross-head speed were used in all experiments. Overall, 65% relative humidity and 20 °C were maintained during the measurement. The maximum force to break the adhesive area was recorded. The adhesive strength was calculated by dividing the force by the glue area.

Amino Acid Analysis. To determine the amount of protein remaining on the glue area, amino acid analysis was used. The glue area (~1 cm²) was cut from the lap shear sample and the top and bottom parts were separately hydrolyzed in 6 M HCl (Merck), containing 0.1% phenol (Sigma-Aldrich) at 110 °C for 24 h. L-norleucine (Sigma-Aldrich) was used as an internal standard. After the hydrolysis, the solution was filtered to remove the ash and the acid was evaporated. The remaining sample was resuspended according to the system protocol (Sykam GmbH). The solution was collected, centrifuged, filtered, and the supernatant was analyzed with an amino acid analyzer (S433, Sykam GmbH) with a UV detector at 570 nm and 440 nm. Protein amounts were calculated based on the internal standard and the protein sequence. Glycine, alanine, glutamine, and

glutamic acid were used for the concentration determination since they are most abundant in the protein and therefore most reliable. For BSA samples, aspartic acid, glutamic acid, leucine, and lysine were used for the concentration determination.

Tritium Labeling of CBM-eADF3-CBM. Tritium labeling of CBM-eADF3-CBM for autoradiography was carried out with [³H]N-succinimidylpropionate ([³H]-NSP) (Novandi). Further, 5 mCi (185 MBq) of [³H]-NSP stored in a heptane:ethyl acetate solution (3:2) was used. Most of the solvent was evaporated using a nitrogen stream. The concentrated solution was mixed with 9 ml of a protein solution at pH 9.3. The concentration of the protein solution was 1.8 g L⁻¹. The solution was mixed at room temperature for 4 h. The unreacted label was removed with Econo-Pac 10 DG desalting columns (Bio-Rad), and the final activity was determined by a liquid scintillation counter.

Autoradiography. Protein distribution in delignified cellulose was studied with ³H-autoradiography. Veneer samples were prepared exactly the same way as described above, but for this purpose, a mixture of CBM-eADF3-CBM with and without a tritium label was used and the sample was not cut into 1 cm wide strips. The mixture was prepared in such a ratio that 2.6 MBq activity was obtained. Autoradiographic imaging was performed with a Fujifilm FLA 5100 reader and an IP S imaging mode. A 635 nm laser, 16-bit gradation, and 10 μm resolution were used. A Fujifilm BAS-TR2025 film was used for imaging. The veneer layers were separated from each other and they were exposed for 24 h prior to imaging. Both sides of the veneer samples were imaged.

Liquid Scintillation Counting. To quantify labeled protein, we used liquid scintillation counting (Hidex 300 SL). To determine the protein content in veneer samples, cellulose was hydrolyzed with a Cellic CTec2 cellulase mixture (Merck) prior to measurement. Hydrolysis was carried out in 0.1 M sodium citrate buffer at pH 4.8 and 50 °C for 7 days. Overall, 8 mL of buffer and 15 μL of cellulase were used per cellulose sample. An Ultima Gold scintillation cocktail (PerkinElmer) was used for sample preparation in all cases.

Scanning Electron Microscopy (SEM). Electron microscopy imaging was carried out with a Zeiss Sigma FE-SEM with variable pressure. A secondary electron detector and 1.5 kV EHT were used. Samples were coated with a 7 nm platinum/palladium mixture prior to imaging. Fracture surfaces were imaged after mechanical testing. Both layers were imaged separately. Samples of CBM-eADF3-CBM condensates were prepared by stretching a semidry protein film made from a phase-separated protein solution and then imaging the cracks induced to the film.

Rheology. Zero-shear viscosities of starch, BSA, and CBM-eADF3-CBM samples were measured at 23 °C with a rheometer (MCR 302, Anton Paar) using a CP50-1 measurement tool and a 0.1 mm gap size. The samples were prepared identical to those used for lap shear measurements. Shear rate sweep was carried out in the range 0.0001–10 s⁻¹. The measurement point duration was selected as set by the device. The point density was 5 pt per decade.

RESULTS AND DISCUSSION

The wet and freshly delignified veneer has poor mechanical integrity and falls apart very easily. The vacuum compression method proved overall to be practical for preparing samples. Upon compression and drying, the delignified veneers became rigid and strong. Properties of single sheets of delignified veneer were initially analyzed. They had an ultimate strength of 218 ± 37 MPa, Young's modulus of 10.5 ± 1.3 GPa, and a strain-to-failure value of 2.8 ± 0.6%. These values are comparable to materials based on compressed micro- or nanofibrillated cellulose.²⁸ The delignified and compressed veneer is reminiscent of such nanofibrillated cellulose materials, in that the adhesion between fibrils is probably very similar and based on the general high binding of cellulose fibrils to each other when aligned.^{28,29} This binding interaction is generally thought to be based on hydrogen bonds and

London dispersion forces.³⁰ The good mechanical properties of the delignified veneers also suggest that the ultrastructure and alignment give a good interface for interaction between components and do not exhibit microscale aggregation or disruption of structures that would lead to weak interfaces within the material.⁶

Using the engineered silk protein CBM-eADF3-CBM as an adhesive (Scheme 1), lap joints between veneers showed excellent results with adhesive strengths of 6.7 MPa on average and up to 10 MPa for individual samples ($N = 35$) (Figure 1).

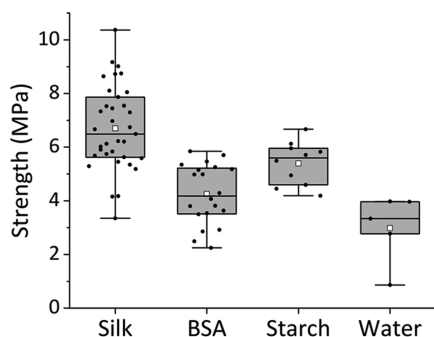


Figure 1. Box plot of the adhesion strength of the engineered silk protein CBM-eADF3-CBM; the references BSA, starch, and a blank control with only water. The mean is shown as a white square and the box shows lines at 25th, 50th, and 75th percentiles. Whiskers show maximum and minimum values. Welch's *t*-test shows a *p*-value of 4.1×10^{-8} for the comparison between silk and BSA and 0.001 between silk and starch or water.

Some samples had lower performance, even down to 3.3 MPa. Detailed visual observations showed that there was a clear correlation between strength and features of fracture surfaces (Figure 2). Sets of samples with high strengths, roughly 8–10 MPa, showed smooth fracture surfaces, whereas samples breaking at lower forces, below 6 MPa, showed large tear-outs of cellulose fibers. Over multiple series of samples, the surfaces showed consistently the same features, i.e., stronger samples showed only little tear-out and for weaker samples, there was clearly much more tear-out. At higher magnification using scanning electron microscopy (SEM), it could be seen

that even the seemingly smooth surface of the highest strength samples did present a low degree of near-interfacial tear-out.

Reference samples were made with BSA protein, starch, and by leaving out the adhesive. In the latter case, when leaving out the adhesive, the same volume of water was applied instead to find the background adhesiveness of cellulose. These were termed blank samples (Figure 1). Leaving out the adhesive in the blank samples gave lap shear strengths of 2.9 MPa on average ($N = 5$). This high base level of adhesion can be understood by the inherent cohesiveness of cellulose with itself as discussed above for the compressed delignified veneers themselves.³⁰ The wet delignified cellulose is easily deformed and allows good contact between the cellulose fibrils when compressed. Both starch and BSA showed intermediate values between the silk and the blank samples, with average strengths of 5.4 MPa ($N = 10$) and 4.2 MPa ($N = 20$), respectively. As another type of reference, we also used nondelignified veneers, i.e., the untreated native wood as an adherend. The resulting joints were too weak to be measured reliably. We did not continue to study them nor alternative ways of preparing native wood samples.

Of the reference samples, we found that starch gave overall the largest tear-outs of the cellulose adherend, even greater than the weakest samples using silk (Figure 3). BSA samples showed similar smoothness as the strongest silk samples. The blank control sample gave rougher surfaces than the BSA samples but had much less tear-out than the starch samples. In none of the samples, we could identify a clear bond line thickness by microscopy. The reason for this is most likely that the adhesives were easily compressible and used in relatively small amounts, and thus did not form assemblies or structures at the interfaces in such amounts that could be visibly detected.

For a further understanding of the systems, we compared strength to the strain at which samples failed and to the initial stiffness of the different samples (Figure 4). Generally, stronger samples showed a higher strain when breaking. However, BSA samples showed more strain than silk and starch for similar strengths (Figure 4A). Silk samples showed the highest combination of strength and strain. BSA generally allowed for more extension in the sample before failure at corresponding strengths compared to silk and starch. In Figure 4B, we note that the stiffness of the samples showed a quite

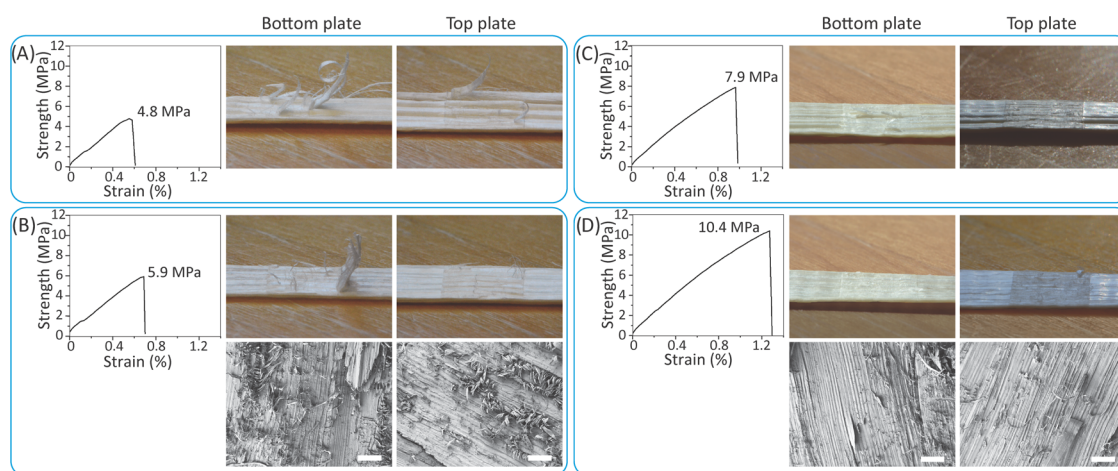


Figure 2. Representative data of samples with silk adhesive showing different lap shear strengths. The ultimate strengths are (A) 4.8 MPa, (B) 5.9 MPa, (C) 7.9 MPa, and (D) 10.4 MPa. Details of SEM images are shown for sets B and D. The scale bar is 200 μm . The SEM images also show how well the ultrastructure of the wood remained intact throughout the delignification and compression process.

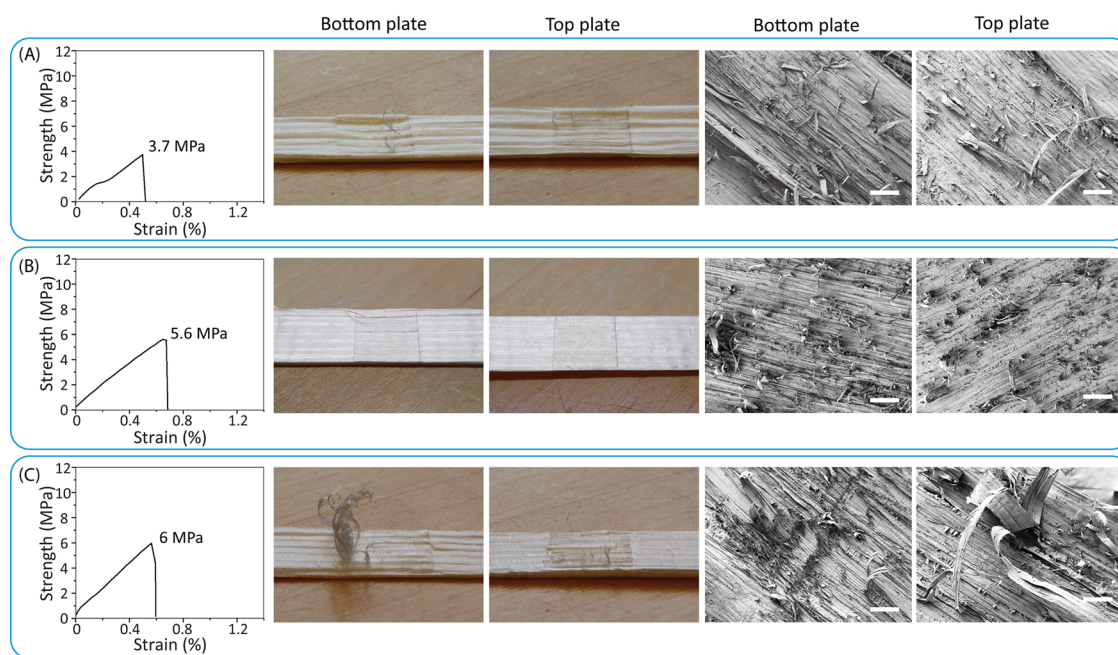


Figure 3. Representative examples of reference experiments. (A) Blank sample with only water, (B) BSA, and (C) starch as adhesives. BSA samples showed very little tear-out, starch a high degree of tear-out, while the blank control sample showed intermediate levels of tear-out. The scale bar in SEM images is 200 μm .

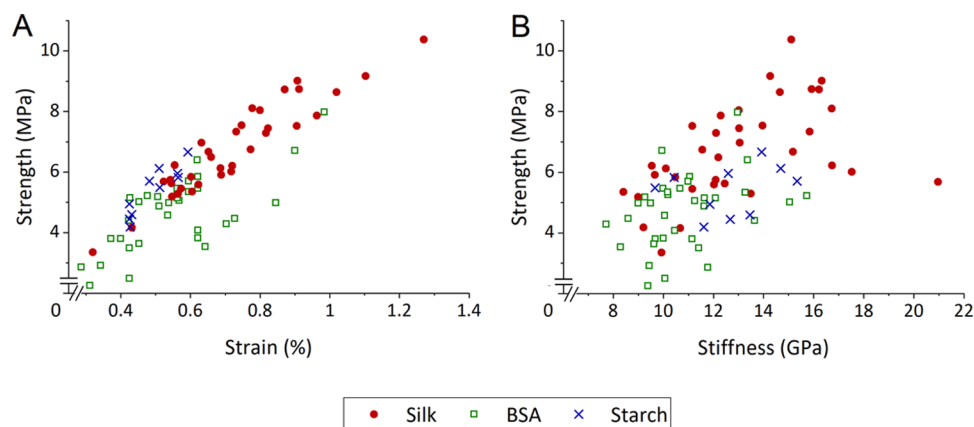


Figure 4. (A) Strain-at-break compared to the strength of the lap joint for silk, BSA, and starch samples. (B) Initial stiffness of the sample compared to the strength of the lap joint.

large variability, with no clear trend. However, overall many silk samples showed a higher stiffness than samples with other adhesives. The stiffness was calculated using initial data points of the stress–strain curve, i.e., prior to adhesive failure.

We next analyzed the amount of protein retained within the lap joint, as the sample preparation method could lead to the spreading of adhesive away from the bonding area. Total hydrolysis of the samples and subsequent amino acid quantification were performed (Figure 5). Only 1–4 mg of the silk protein and 1–2 mg of BSA were retained in the lap joint area, representing less than 20% of the applied amount. In neither case was there a significant correlation between the amount of the adhesive and strength. Experiments where the applied amount of silk protein was increased fourfold showed no effect on the amount of protein retained nor on mechanical properties. The amount of protein relative to cellulose was between 0.5 and 2%, Although the amount appears low, it is of the same magnitude that is found in, e.g., the proteinaceous

matrix of nacre.¹¹ This is in line with the common understanding that the amount of the adhesive is typically not a critical parameter for mechanisms of adhesion.³¹ Remaining at the interface, the applied amount of starch has been shown to affect performance, and has been optimized previously.²⁷

To understand the spreading of CBM-eADF3-CBM in the cellulose matrix, we analyzed the distribution of protein in the samples. For this, we used ³H-radiolabeled CBM-eADF3-CBM and analyzed the spreading of the protein in the sample by both autoradiography and liquid scintillation counting. For autoradiography, the sample preparation was done in exactly the same way as for the regular sample, except that the veneer was not cut into test strips. Instead, after drying, the two veneer sheets were separated from each other and placed on the autoradiography screen (Figure 6A). We noted that the protein spread in an irregular fashion along the wood fibers when analyzing the interior surface, i.e., that turned inward in

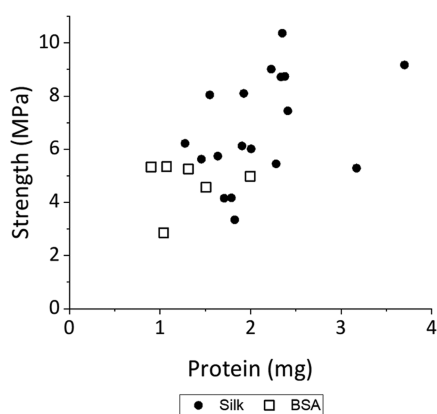


Figure 5. Lap shear strength as a function of protein that was retained in the 1 cm² glue area. Good adhesion could be achieved even with low amounts of protein. The protein amount was determined using amino acid analysis.

the sample preparation. We detected only a little protein on the exterior surface, indicating that there was only little penetration of protein through thickness of the cellulose. This indicates that the protein does not easily impregnate the full thickness of the veneer and that capillary forces transport protein away from the site of application.

After the autoradiograph scan, the veneer was cut into 1 cm² pieces. The cellulose was liquified by hydrolysis using a cellulase mixture after which the labeled protein was quantified by liquid scintillation counting. The spreading of the protein is shown as a heatmap in Figure 6B. We can conclude that only approximately 20% of the CBM-eADF3-CBM protein stayed within the bonding area. The remaining protein spread along the fiber direction so that about 40% was found within 1 cm of

the applied region and the rest had spread outside that. We also noted that along the gluing area, there was variability in how the protein had spread.

To better understand the properties of CBM-eADF3-CBM as an adhesive, we measured its viscosity using oscillatory and rotational rheology measurements. We found that its viscosity was highly variable between samples, although sample preparation was done similarly. The zero-shear viscosity showed a broad range of 3–2300 Pa·s at concentrations between 94 and 124 gL⁻¹. The high values and the variability can both probably be ascribed to the coacervated state of the protein, as the coacervate droplets are viscous and also showed variability in their size between samples (Figure 7). As a comparison, a 80 gL⁻¹ BSA solution had a significantly lower zero-shear viscosity range of 2–5 Pa·s. The starch paste at 16.5 wt % showed much high zero-shear viscosity values in the range of 5000–12 000 Pa·s (see the Supporting Information).

The use of lap shear testing to compare adhesives requires caution as they are affected by parameters such as bending and strain distribution that may vary significantly between systems.³¹ Ductility of both adherend and adhesive affects results greatly.³² For this reason, standardized testing procedures are generally useful to enable comparison between adhesives. However, for the delignified cellulose system under study here, no standard systems are available as it is a new experimental system. Earlier, BSA and recombinant spider silk were compared in a system in which glass was used as an adherend. In that study, BSA outperformed recombinant spider silk as an adhesive (8.3 MPa for BSA, 6.2 MPa for silk).²⁶ However, both adhesives were very weak on less stiff adherends. A direct comparison to the present system is, therefore, difficult as glass is stiff with Young's modulus around 50 GPa, while the delignified and compressed cellulose here

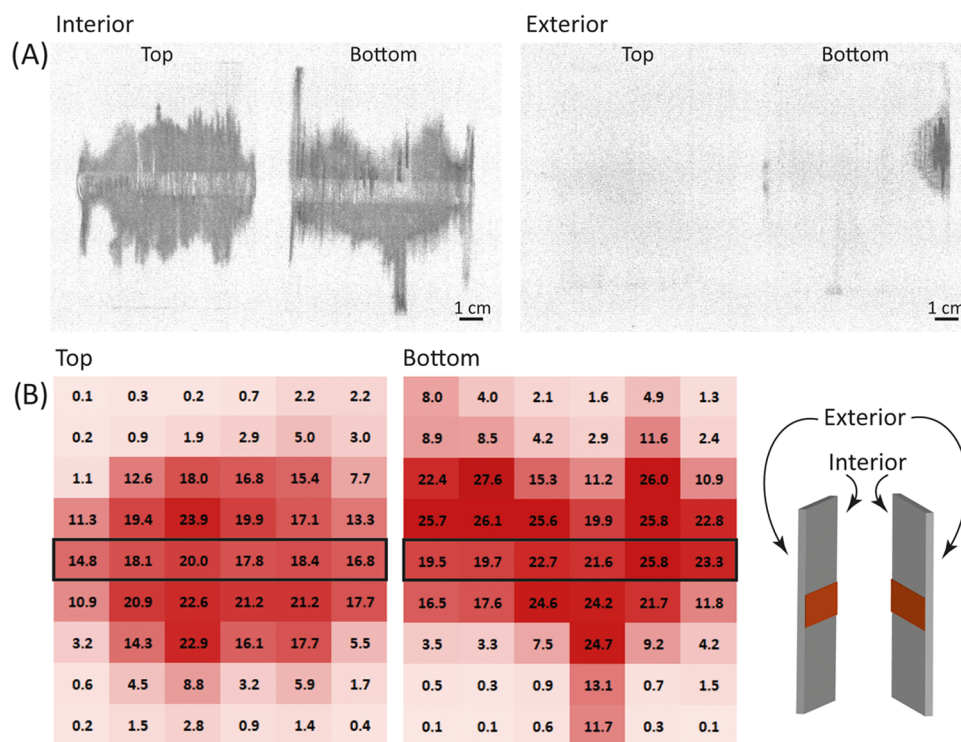


Figure 6. (A) ³H-autoradiographs of the veneer sheets showing the spread of protein. (B) Heatmap showing the spread of protein within the veneer sheets. Values represent the radioactivity in kBq measured from each cm². The glue area is indicated with a square.

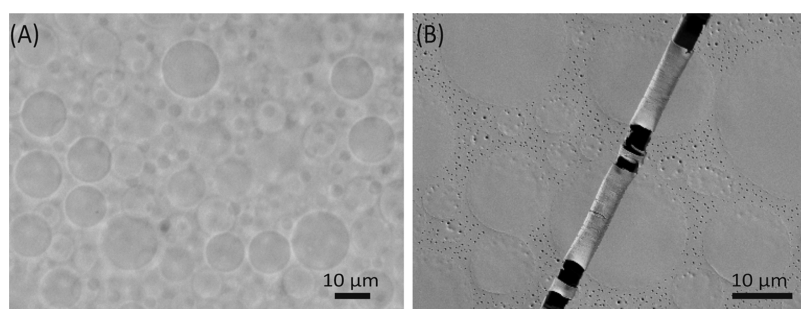
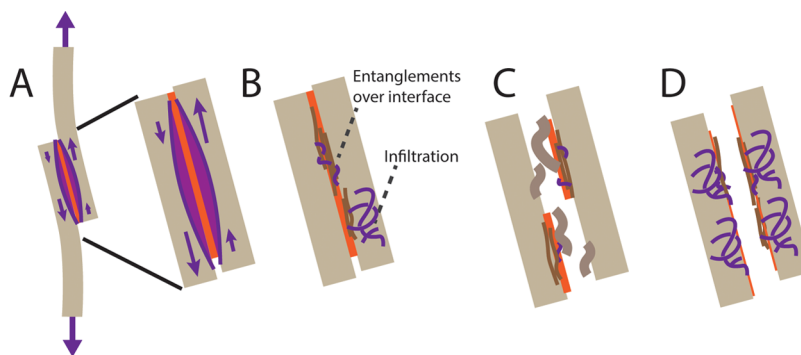


Figure 7. (A) Optical micrograph of the appearance of a typical sample of CBM-eADF3-CBM before application onto the gluing area, showing the coacervated state of the protein. (B) SEM images of CBM-eADF3-CBM coacervates that had been stretched after allowing most of the water to evaporate, resulting in a crack. Bridging over the cracks through coacervates shows a tear-out of protein and suggests interactions or entanglements of the proteins.

Scheme 2. Mechanisms in Lap Shear Testing^a



^a(A) In the lap shear test, the uneven strain in the adherend creates stresses within the interfacial region and within the adherend. (B) In particular, two mechanisms are important for the strength of the lap joint: entanglements over the interface and adhesive infiltration. (C) Poor infiltration can lead to large strains in the near interfacial region and a weak bond. A large tear-out would result. (D) A good infiltration can strengthen the near interfacial region leading to adhesive failure in the interface and little tear-out.

was around 10 GPa. A number of other details, such as processing, also suggest that different mechanisms were at play. For a very stiff adherend such as glass, a highly cross-linked and brittle adhesive can give excellent strength. In one extreme example, very stiff cellulose nanocrystals were carefully assembled as an adhesive layer between two glass slides giving a high lap strength of 7 MPa. Consequently, due to the high stiffness of the system, the bonding was extremely brittle, breaking at less than 0.08 MPa if the force was applied from the side.³³ Therefore, such a system would be expected to be very weak on a more easily yielding adherend.

In another study with similar goals, cross-linking chemistry was used to improve BSA as an adhesive for wood.³⁴ Without cross-linking, BSA gave a strength of 0.1 MPa, and when optimized with cross-linkers, the adhesion increased to 4 MPa. However, direct comparisons with the current study are difficult since so many factors, in particular, the adherend, differ. We also note that in our current study, testing wood as the adherend gave very low strength. The reason for these results remained unexplored but could be that wood requires better cohesion in the adhesive over larger distances due to irregularities in its structure. Nonetheless, we note that there are several reports in which a variety of adherends and optimizations of treatments show a good potential of proteins.³⁵ Of protein-based adhesives, soy protein has been studied extensively (2–8 MPa).^{34,36,37} The highest values are typically obtained in cross-linked systems, with examples

including modified BSA (4 MPa),³⁴ gluten (2 MPa),³⁸ corn zein (8 MPa),³⁹ and starch (7.8 MPa).⁴⁰

In the current work, as the adherend is not very stiff, it is expected that the adhesive should show deformability to accommodate for strain in the sample.³² Such strain occurs in the lap joint because of the distortion of the sample at the joint due to, e.g., adherend stretching.³¹ Effects of infiltration of the near interfacial region have been discussed in the literature and are generally seen as leading to an off-loading of the lap joint because forces are more evenly distributed due to the adhesive penetration.⁴¹ Starch is a stiffer molecule than BSA and has more extended polymer chains and much higher viscosity. The high observed tear-out for starch indicates that although it did bind strongly, and it did not infiltrate the adherend. This is expected since the molecular mass of starch is high. It is likely that it formed a surface layer that pulled out cellulose fibrils from the adhered upon failure. BSA with its smaller molecular size and low viscosity could infiltrate the adherend, resulting in cohesiveness within the near interfacial region of the adherend. Because cellulose fibrils are more closely packed, better cohesion would form within the near interfacial region compared to the joint interface. This is because the interface between adherends does not have equally good packing and alignment of cellulose fibrils as within the adherend, leading to larger gaps and longer bonding distances. Hence, BSA would show low tear-out upon failure.

The large differences in tear-out between high and low-strength silk samples suggest a shift in the mechanism of

adhesive failure between the samples. In general, it has been suggested that for polymeric adhesives, chain entanglements are critical for forming good contacts over the interface and creating good cohesiveness.^{25,42–44} In Scheme 2, we summarize our interpretation of the underlying mechanisms. It seems likely that in the high-strength samples, silk had been able to both infiltrate the adherend sufficiently and at the same time provide a good cohesion over the interface. In the low-strength samples, it seems that infiltration below the interface was insufficient in comparison. This hypothesis is supported by the noted high tear-out and the finding that silk could sometimes show a high viscosity. We, therefore, find it possible that the large tear-out in the weakest CBM-eADF3-CBM silk samples resulted from a failure to create bonding below the interface, i.e., in the near interfacial region. Upon the failure of these weaker samples, a fairly large tear-out results as the bridging of the interface would be relatively strong, but the low infiltration led to the failure of fiber interactions deeper inside the cellulose adherend (Scheme 2C). Even with low infiltration, they could give a cohesive bridging over the interface, possibly supported by the molecular entanglement to which coacervation and relatively long chain lengths lead (Figure 7). The strongest silk samples would then have achieved a good infiltration beneath the interfacial region as well as provided good bridging over the interface, resulting in a smooth fracture surface and an overall strong bond (Scheme 2D).

The reasons for the relatively large variability in adhesive strength of the CBM-eADF3-CBM silk adhesive samples remained unclear but can be related to the very broad range of viscosity that different silk samples showed. Previously, it has been shown that the viscosity is dependent on the phase separation of the silk protein due to intermolecular interactions between the silk molecules.²² Furthermore, viscosity of coacervates has also in other contexts been proposed as means of regulating the extent of protein infiltration into porous scaffolds.⁴⁵ Unfortunately, in our setup, it was not possible to measure the viscosity of silk used in each experiment since even application on the rheometer and removal could result in irreproducible processing of the protein. Also, gelling and precipitation occurred, rendering samples unusable. Therefore, a technical problem is the unpredictability of exactly how and at which stage the viscosity of the coacervated CBM-eADF3-CBM sample changed.

CONCLUSIONS

In conclusion, we have shown how recombinant silk protein in combination with delignified wood forms a strong adhesive system. The work shows a direction for future materials in which we utilize natural components to a maximal extent, but in a way that processing could be scaled and performed industrially. In particular, the adhesive processing system was fully aqueous. We have only recently gained an understanding of how the assembly of recombinant proteins on a molecular level can be controlled²⁰ and we highlight the potential of using them for new materials. The work also relies on the underlying work on understanding how biological materials, in particular, composite structures, function.^{1,43} The potential advantage is simplicity; we used no cross-linkers or other modifiers. The work highlights that high performance can be obtained in fully biobased approaches with aqueous processability as will be required for future sustainable materials with a low environmental burden. We see an opportunity in

continued structural modification of the recombinant protein to further enhance its properties.

ASSOCIATED CONTENT

Supporting Information

The Supporting Information is available free of charge at <https://pubs.acs.org/doi/10.1021/acssuschemeng.1c07043>.

Data from rheological characterizations of CBM-eADF3-CBM, starch, and BSA adhesives (PDF)

AUTHOR INFORMATION

Corresponding Author

Markus B. Linder – Department of Bioproducts and Biosystems, Aalto University, 02150 Espoo, Finland;

orcid.org/0000-0002-7271-6441;

Email: markus.linder@aalto.fi

Authors

Laura Lemetti – Department of Bioproducts and Biosystems, Aalto University, 02150 Espoo, Finland; orcid.org/0000-0003-1845-752X

Jennifer Tersteegen – Department of Bioproducts and Biosystems, Aalto University, 02150 Espoo, Finland;

orcid.org/0000-0002-7356-0186

Juuso Sammaljärvi – Department of Chemistry, University of Helsinki, 00014 Helsinki, Finland

A. Sesilja Aranko – Department of Bioproducts and Biosystems, Aalto University, 02150 Espoo, Finland;

orcid.org/0000-0001-9425-3524

Complete contact information is available at:

<https://pubs.acs.org/doi/10.1021/acssuschemeng.1c07043>

Funding

This work was performed within the project “Strong Composite” supported under the umbrella of ERANET Cofund ForestValue, funded by Academy of Finland projects #308772, #317395, #326345, and #333238. The authors are grateful for the support by the FinnCERES Materials Bioeconomy Ecosystem, the Bioeconomy Infrastructure, and the OtaNano—Nanoscience Center (Aalto-NMC) at Aalto University.

Notes

The authors declare no competing financial interest.

ACKNOWLEDGMENTS

The authors thank professor Ingo Burgert and his team at ETH Zürich for helping us to establish delignification and compression setups. They also thank Dr. Isabell Tunn for help with rheology measurements and Teemu Väiläsalmi for help with Welch's test.

REFERENCES

- (1) Wegst, U. G. K.; Bai, H.; Saiz, E.; Tomsia, A. P.; Ritchie, R. O. Bioinspired Structural Materials. *Nat. Mater.* **2015**, *14*, 23–36.
- (2) Byrne, G.; Dimitrov, D.; Monostori, L.; Teti, R.; van Houten, F.; Wertheim, R. Biologicalisation: Molecular Transformation in Manufacturing. *CIRP J. Manuf. Sci. Technol.* **2018**, *21*, 1–32.
- (3) Li, T.; Chen, C.; Brozina, A. H.; Zhu, J. Y.; Xu, L.; Driemeier, C.; Dai, J.; Rojas, O. J.; Isogai, A.; Wågberg, L.; Hu, L. Developing Fibrillated Cellulose as a Sustainable Technological Material. *Nature* **2021**, *590*, 47–56.
- (4) Heise, K.; Kontturi, E.; Allahverdiyeva, Y.; Tammelin, T.; Linder, M. B.; Nonappa, Ikkala, O. Nanocellulose: Recent Fundamental

Advances and Emerging Biological and Biomimicking Applications. *Adv. Mater.* **2021**, *33*, No. 2004349.

(5) Frey, M.; Widner, D.; Segmehl, J. S.; Casdorff, K.; Keplinger, T.; Burgert, I. Delignified and Densified Cellulose Bulk Materials with Excellent Tensile Properties for Sustainable Engineering. *Appl. Mater. Interfaces* **2018**, *10*, 5030–5037.

(6) Frey, M.; Schneider, L.; Masania, K.; Keplinger, T.; Burgert, I. Delignified Wood–Polymer Interpenetrating Composites Exceeding the Rule of Mixtures. *ACS Appl. Mater. Interfaces* **2019**, *11*, 35305–35311.

(7) Frey, M.; Zirkelbach, M.; Dransfeld, C.; Faude, E.; Trachsel, E.; Hannus, M.; Burgert, I.; Keplinger, T. Fabrication and Design of Wood-Based High-Performance Composites. *J. Vis. Exp.* **2019**, *153*, No. e60327.

(8) Frey, M.; Biffi, G.; Adobes-Vidal, M.; Zirkelbach, M.; Wang, Y.; Tu, K.; Hirt, A. M.; Masania, K.; Burgert, I.; Keplinger, T. Tunable Wood by Reversible Interlocking and Bioinspired Mechanical Gradients. *Adv. Sci.* **2019**, *6*, No. 1802190.

(9) Pönni, R.; Kontturi, E.; Vuorinen, T. Accessibility of Cellulose: Structural Changes and Their Reversibility in Aqueous Media. *Carbohydr. Polym.* **2013**, *93*, 424–429.

(10) Sutherland, T. D.; Young, J. H.; Weisman, S.; Hayashi, C. Y.; Merritt, D. J. Insect Silk: One Name, Many Materials. *Annu. Rev. Entomol.* **2010**, *55*, 171–188.

(11) Smith, B. L.; Schäffer, T. E.; Viani, M.; Thompson, J. B.; Frederick, N. A.; Kindt, J.; Belcher, A.; Stucky, G. D.; Morse, D. E.; Hansma, P. K. Molecular Mechanistic Origin of the Toughness of Natural Adhesives, Fibres and Composites. *Nature* **1999**, *399*, 761–763.

(12) Pasche, D.; Horbelt, N.; Marin, F.; Motreuil, S.; Fratzl, P.; Harrington, M. J. Self-Healing Silk from the Sea: Role of Helical Hierarchical Structure in Pinna Nobilis Byssus Mechanics. *Soft Matter* **2019**, *15*, 9654–9664.

(13) Sahni, V.; Blackledge, T. A.; Dhinojwala, A. A Review on Spider Silk Adhesion. *J. Adhes.* **2011**, *87*, 595–614.

(14) Huemmerich, D.; Helsen, C. W.; Quedzuweit, S.; Oschmann, J.; Rudolph, R.; Scheibel, T. Primary Structure Elements of Spider Dragline Silks and Their Contribution to Protein Solubility. *Biochemistry* **2004**, *43*, 13604–13612.

(15) Mohammadi, P.; Aranko, A. S.; Landowski, C. P.; Ikkala, O.; Jaudzems, K.; Wagermaier, W.; Linder, M. B. Biomimetic Composites with Enhanced Toughening Using Silk-Inspired Triblock Proteins and Aligned Nanocellulose Reinforcements. *Sci. Adv.* **2019**, *5*, No. eaaw2541.

(16) Sun, Y.; Lim, Z. W.; Guo, Q.; Yu, J.; Miserez, A. Liquid–Liquid Phase Separation of Proteins and Peptides Derived from Biological Materials: Discovery, Protein Engineering, and Emerging Applications. *MRS Bull.* **2020**, *45*, 1039–1047.

(17) Waite, J. H. Mussel Adhesion – Essential Footwork. *J. Exp. Biol.* **2017**, *220*, 517–530.

(18) Hagn, F.; Eisoldt, L.; Hardy, J. G.; Vendrely, C.; Coles, M.; Scheibel, T.; Kessler, H. A Conserved Spider Silk Domain Acts as a Molecular Switch That Controls Fibre Assembly. *Nature* **2010**, *465*, 239–242.

(19) Askarieh, G.; Hedhammar, M.; Nordling, K.; Saenz, A.; Casals, C.; Rising, A.; Johansson, J.; Knight, S. D. Self-Assembly of Spider Silk Proteins Is Controlled by a PH-Sensitive Relay. *Nature* **2010**, *465*, 236–238.

(20) Mohammadi, P.; Aranko, A. S.; Lemetti, L.; Cenev, Z.; Zhou, Q.; Virtanen, S.; Landowski, C. P.; Penttilä, M.; Fischer, W. J.; Wagermaier, W.; Linder, M. B. Phase Transitions as Intermediate Steps in the Formation of Molecularly Engineered Protein Fibers. *Commun. Biol.* **2018**, *1*, No. 86.

(21) Griffo, A.; Rooijackers, B. J. M.; Hähl, H.; Jacobs, K.; Linder, M. B.; Laaksonen, P. Binding Forces of Cellulose Binding Modules on Cellulosic Nanomaterials. *Biomacromolecules* **2019**, *20*, 769–777.

(22) Mohammadi, P.; Beaune, G.; Stokke, B. T.; Timonen, J. V. I.; Linder, M. B. Self-Coacervation of a Silk-Like Protein and Its Use As

an Adhesive for Cellulosic Materials. *ACS Macro Lett.* **2018**, *7*, 1120–1125.

(23) Batys, P.; Fedorov, D.; Mohammadi, P.; Lemetti, L.; Linder, M. B.; Sammalkorpi, M. Self-Assembly of Silk-like Protein into Nanoscale Bicontinuous Networks under Phase-Separation Conditions. *Biomacromolecules* **2021**, *22*, 690–700.

(24) Fedorov, D.; Batys, P.; Hayes, D. B.; Sammalkorpi, M.; Linder, M. B. Analyzing the Weak Dimerization of a Cellulose Binding Module by Analytical Ultracentrifugation. *Int. J. Biol. Macromol.* **2020**, *163*, 1995–2004.

(25) Raos, G.; Zappone, B. Polymer Adhesion: Seeking New Solutions for an Old Problem. *Macromolecules* **2021**, DOI: 10.1021/acs.macromol.1c01182.

(26) Roberts, A. D.; Finnigan, W.; Kelly, P. P.; Faulkner, M.; Breitling, R.; Takano, E.; Scrutton, N. S.; Blaker, J. J.; Hay, S. Non-Covalent Protein-Based Adhesives for Transparent Substrates—Bovine Serum Albumin vs. Recombinant Spider Silk. *Mater. Today Bio.* **2020**, *7*, No. 100068.

(27) Frey, M.; Schneider, L.; Razi, H.; Trachsel, E.; Faude, E.; Koch, S. M.; Masania, K.; Fratzl, P.; Keplinger, T.; Burgert, I. High-Performance All-Bio-Based Laminates Derived from Delignified Wood. *ACS Sustainable Chem. Eng.* **2021**, *9*, 9638–9646.

(28) Li, K.; Clarkson, C. M.; Wang, L.; Liu, Y.; Lamm, M.; Pang, Z.; Zhou, Y.; Qian, J.; Tajvidi, M.; Gardner, D. J.; Tekinalp, H.; Hu, L.; Li, T.; Ragauskas, A. J.; Youngblood, J. P.; Ozcan, S. Alignment of Cellulose Nanofibers: Harnessing Nanoscale Properties to Macroscale Benefits. *ACS Nano* **2021**, *15*, 3646–3673.

(29) Ansari, F.; Berglund, L. A. Toward Semistructural Cellulose Nanocomposites: The Need for Scalable Processing and Interface Tailoring. *Biomacromolecules* **2018**, *19*, 2341–2350.

(30) Nishiyama, Y. Molecular Interactions in Nanocellulose Assembly. *Philos. Trans. R. Soc. Math. Phys. Eng. Sci.* **2018**, *376*, No. 20170047.

(31) Abbott, S. *Adhesion Science: Principles and Practice*; Destech Publications: Lancaster, USA.

(32) Mazzotta, M. G.; Putnam, A. A.; North, M. A.; Wilker, J. J. Weak Bonds in a Biomimetic Adhesive Enhance Toughness and Performance. *J. Am. Chem. Soc.* **2020**, *142*, 4762–4768.

(33) Tardy, B. L.; Richardson, J. J.; Greca, L. G.; Guo, J.; Ejima, H.; Rojas, O. J. Exploiting Supramolecular Interactions from Polymeric Colloids for Strong Anisotropic Adhesion between Solid Surfaces. *Adv. Mater.* **2020**, *32*, No. 1906886.

(34) Román, J. K.; Wilker, J. J. Cooking Chemistry Transforms Proteins into High-Strength Adhesives. *J. Am. Chem. Soc.* **2019**, *141*, 1359–1365.

(35) Imam, S. H.; Bilbao-Sainz, C.; Chiou, B.-S.; Glenn, G. M.; Orts, W. J. Biobased Adhesives, Gums, Emulsions, and Binders: Current Trends and Future Prospects. *J. Adhes. Sci. Technol.* **2013**, *27*, 1972–1997.

(36) Zeng, Y.; Xu, P.; Yang, W.; Chu, H.; Wang, W.; Dong, W.; Chen, M.; Bai, H.; Ma, P. Soy Protein-Based Adhesive with Superior Bonding Strength and Water Resistance by Designing Densely Crosslinking Networks. *Eur. Polym. J.* **2021**, *142*, No. 110128.

(37) Wang, Z.; Zhao, S.; Pang, H.; Zhang, W.; Zhang, S.; Li, J. Developing Eco-Friendly High-Strength Soy Adhesives with Improved Ductility through Multiphase Core–Shell Hyperbranched Polysiloxane. *ACS Sustainable Chem. Eng.* **2019**, *7*, 7784–7794.

(38) Xi, X.; Pizzi, A.; Gerardin, C.; Liao, J.; Amirou, S.; Abdalla, S. Glutaraldehyde–Wheat Gluten Protein Adhesives for Wood Bonding. *J. Adhes.* **2021**, *97*, 88–100.

(39) Schmidt, G.; Woods, J. T.; Fung, L. X. B.; Gilpin, C. J.; Hamaker, B. R.; Wilker, J. J. Strong Adhesives from Corn Protein and Tannic Acid. *Adv. Sustainable Syst.* **2019**, *3*, No. 1900077.

(40) Zhang, Y.; Ding, L.; Gu, J.; Tan, H.; Zhu, L. Preparation and Properties of a Starch-Based Wood Adhesive with High Bonding Strength and Water Resistance. *Carbohydr. Polym.* **2015**, *115*, 32–37.

(41) Averina, E.; Konnerth, J.; D’Amico, S.; van Herwijnen, H. W. G. Protein Adhesives: Alkaline Hydrolysis of Different Crop Proteins

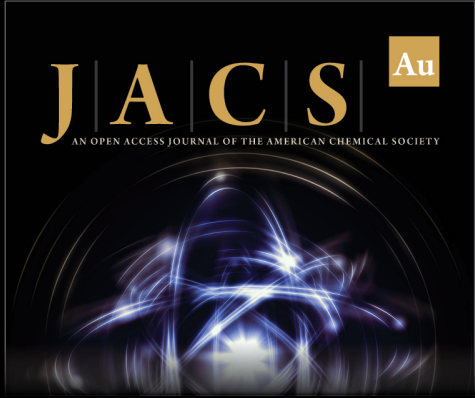
as Modification for Improved Wood Bonding Performance. *Ind. Crops Prod.* **2021**, *161*, No. 113187.

(42) Fratzl, P.; Burgert, I.; Gupta, H. S. On the Role of Interface Polymers for the Mechanics of Natural Polymeric Composites. *Phys. Chem. Chem. Phys.* **2004**, *6*, 5575–5579.


(43) Studart, A. R. Towards High-Performance Bioinspired Composites. *Adv. Mater.* **2012**, *24*, 5024–5044.


(44) Wool, R. P. Polymer Entanglements. *Macromolecules* **1993**, *26*, 1564–1569.


(45) Tan, Y.; Hoon, S.; Guerette, P. A.; Wei, W.; Ghadban, A.; Hao, C.; Miserez, A.; Waite, J. H. Infiltration of Chitin by Protein Coacervates Defines the Squid Beak Mechanical Gradient. *Nat. Chem. Biol.* **2015**, *11*, 488–495.



JACS Au
AN OPEN ACCESS JOURNAL OF THE AMERICAN CHEMICAL SOCIETY

 Editor-in-Chief
Prof. Christopher W. Jones
Georgia Institute of Technology, USA

Open for Submissions 

pubs.acs.org/jacsau  ACS Publications
Most Trusted. Most Cited. Most Read.